



Epigenetic landscape analysis of lncRNAs in acute myeloid leukemia with DNMT3A mutations

Yu-Jun Dai^{1,2,3#}, Fang Hu^{1,2,3#}, Si-Yuan He^{4#}, Yue-Ying Wang⁵

¹Department of Hematologic Oncology, Sun Yat-sen University Cancer Center, Guangzhou 510000, China; ²Center State Key Laboratory of Oncology in South China, Guangzhou 510000, China; ³Collaborative Innovation Center for Cancer Medicine, Guangzhou 510000, China; ⁴The University of Texas MD Anderson Cancer Center UTHealth Graduate School of Biomedical Sciences, Houston, TX 77030, USA; ⁵State Key Laboratory of Medical Genomics, Shanghai Institute of Hematology, Ruijin Hospital, Shanghai Jiao Tong University School of Medicine, Shanghai 200025, China

Contributions: (I) Conception and design: YJ Dai; (II) Administrative support: YY Wang; (III) Provision of study materials or patients: YJ Dai, F Hu, SY He; (IV) Collection and assembly of data: F Hu, SY He; (V) Data analysis and interpretation: YJ Dai, F Hu, SY He; (VI) Manuscript writing: All authors; (VII) Final approval of manuscript: All authors.

[#]These authors contributed equally to the work.

Correspondence to: Yu-Jun Dai. Department of Hematologic Oncology, Sun Yat-sen University Cancer Center, Guangzhou 510000, China.

Email: dgzx16@163.com; Yue-Ying Wang. State Key Laboratory of Medical Genomics, Shanghai Institute of Hematology, Ruijin Hospital, Shanghai Jiao Tong University School of Medicine, Shanghai 200025, China. Email: wyyymoon@hotmail.com.

Background: Acute myeloid leukemia (AML) is a type of cancer that consists of a group of hematological malignancies with high heterogeneity. DNA methyltransferase 3A (*DNMT3A*)-mutated AML patients have a poor prognosis. Some long non-coding RNAs (lncRNAs) have been reported to enhance therapeutic sensitivity, and so could affect the overall survival rate of elderly cytogenetically normal acute myeloid leukemia (CN-AML) patients; however, studies on the lncRNA signature in *DNMT3A*-mutated AML are rare.

Method: The *DNMT3A* R878H conditional knock-in mouse model was constructed to explore the lncRNAs of *DNMT3A* mutation by using the Cuffcomparison method. Cis and trans regulation networks were used to predict candidate genes. The expression levels in leukemic cell lines and the prognostic index of these candidate genes were analyzed with the Broad Institute Cancer Cell Line Encyclopedia (CCLE) and OncoLnc databases. The data for each sample were statistically analyzed using GraphPad Prism.

Results: In this study, we applied the *DNMT3A* R878H conditional knock-in mouse model to explore the lncRNA epigenetic landscape of *DNMT3A* mutation by using the Cuffcomparison method. Twenty-three differentially expressed lncRNAs were identified in *Dnmt3a*^{R878H/WT}Mx1-Cre⁺ mice. We next predicted the downstream targetable genes regulated by these lncRNAs through cis and trans regulation networks and found 124 candidate genes are related to these lncRNAs. In further analysis of 124 genes, we found that increased mRNA expression levels of interleukin 1 receptor type 2 (*IL1R2*), Krüppel-like factor 13 (*KLF13*), ATPase H⁺ transporting V1 subunit A (*ATP6V1A*), proteasome 26S Subunit, non-ATPase 3 (*PSMD3*), and pyrroline-5-carboxylate reductase 2 (*PYCR2*) were associated with poor prognosis in AML. Functional analysis of these genes demonstrated that the pathways involved in autophagy, cell cycle, and hematopoietic stem cell differentiation were more enriched in *Dnmt3a*^{R878H/WT}Mx1-Cre⁺ mice.

Conclusion: Our study was the first to use *DNMT3A* R878H conditional knock-in mouse model to predict the specific lncRNAs regulated by the *DNMT3A* mutation in AML. Six candidate genes were found to be associated with *DNMT3A* mutation with poor prognosis. Our results provided a possible treatment strategy for this disease.

Keywords: lncRNA; *DNMT3A* R878H; knock-in mice; RNA-seq

Submitted Dec 07, 2019. Accepted for publication Feb 04, 2020.

doi: 10.21037/atm.2020.02.143

View this article at: <http://dx.doi.org/10.21037/atm.2020.02.143>

Introduction

DNA methylation, as one of the most important modification methods in epigenetics, plays a key role in the regulation of an organism's life. The mutation frequency of DNA methyltransferase 3A (*DNMT3A*) has been found to be 22.1% in acute myeloid leukemia (AML) (1,2). It has been reported that AML cases with *DNMT3A* mutations are often accompanied by other genetic or epigenetic abnormalities, with nucleophosmin 1 (*NPM1*) mutations (nearly 69.6%) being the most frequent ones. Meanwhile, *MLL* abnormalities are likely exclusive to *DNMT3A* mutations. The *NPM1* gene, which is also one of the most common mutation genes in AML, carries the normal karyotype, with an incidence of approximately 35. *NPM1* mutation is considered to be a relatively favorable prognostic factor in young AML patients but indicates poor survival in older AML patients (3). Studies have shown that *DNMT3A* mutations could be a prognostic factor in *NPM1*-mutated AML with remission (4-6).

DNMT3A and DNA methyltransferase 3 B (*DNMT3B*) jointly control the modification of DNA. They are highly expressed in early mammalian embryos and are gradually down-regulated with cell differentiation, but their expression is low in mature adult tissues (7,8). Animal models have shown that when *DNMT3A* is knocked out during the embryonic stage, mice display growth retardation, dysplasia, and other phenomena, and die by 4 weeks of age (9). *DNMT3A* also plays an important role in maintaining the function of germline stem cells. Knock-out of *DNMT3A* in mouse germ stem cells can cause extensive hypomethylation in the mouse genome and lead to genetic imprinting disorder, spermatogenesis, development disorders, and embryo death in mice (10,11). *DNMT3A* is also a necessary protein for hematopoietic stem cells (HSCs) to maintain their normal proliferation and differentiation function (12,13). Studies have indicated that conditional knockout of *DNMT3A* in mouse HSCs impairs the self-renewal ability of HSCs and destroys their directional differentiation potential (14-16).

As a new mechanism of epigenetic litter control, ncRNA has become a topical issue in modern oncology research. Like many other solid tumors,

the occurrence of hematological malignancies is a disorder of multiple intracellular molecules and multiple links. Studies have shown that long non-coding RNAs (lncRNAs) can control the development of tumors, and notch receptor 1 (*NOTCH1*) has been shown to regulate the expression of several lncRNAs in T-cell acute lymphoblastic leukemia (17). A total of 48 lncRNA patterns have been identified that can predict response to standardized therapy and overall survival in elderly patients with CN-AML (18). Hughes found that in AML patients with a CCAAT enhancer-binding Protein Alpha (*CEBPA*) mutation, the expression of lncRNA Urothelial Cancer-Associated 1 (*UCA1*) was specifically up-regulated, and cell proliferation could be maintained by inhibiting the expression of cell cycle regulator p27kip1 (19). The expression of lncRNA Nuclear Paraspeckle Assembly Transcript 1 (*NEAT1*) in acute promyelocytic leukemia (APL) samples was significantly down-regulated compared with a normal control group and was inhibited by the *PML/RAR α* fusion gene (20). The expression profiles of lncRNAs are related to the recurrent mutation, clinical features, and prognosis of AML (21). Some of these lncRNAs may play a functional role in leukemia formation (22).

Adult leukemia with a *DNMT3A* mutation is mostly insensitive to chemotherapy and has a low remission rate, which is now known as a special subtype of acute leukemia. Thus, our study aimed to explore the specific lncRNAs expressed in *DNMT3A*-mutated leukemia based on a *DNMT3A* mutant mouse model, and analyze the clinical prognosis of its target genes.

Methods

The c-bio portal and metascape analysis

The cBioCancer Genomics Portal was used to analyze the genetic landscape of the *DNMT3A* mutation in The Cancer Genome Atlas (TCGA) AML samples. Detailed clinical information and genetic alternations of *DNMT3A* were provided by this cancer genomic dataset, including 225 tumor research papers. Functional analysis was performed using a web-based portal called Metascape. Clusters enriched terms into groups and were divided by functional

Table 1 Primers for identifying genotype of mice

No.	Primer name	Primer sequence	PCR result
1	Dnmt3a-Loxp-tF:	CAGATGAGCCCACTAGAACCC	Dnmt3a ^{R878H/R878H} : 529 bp; Dnmt3a ^{R878H/WT} : 529+411 bp; Dnmt3a ^{WT/WT} : 411 bp
	Dnmt3a-Loxp-tR:	CCAGCTTTGAGATTCACACTCC	
2	ZMK-2F4:	GCATCGCATTGTCTGAGTAGGTG	Dnmt3a ^{R878H/R878H} : 853 bp; Dnmt3a ^{R878H/WT} : 853 bp; Dnmt3a ^{WT/WT} : 0 bp
	Dnmt3a-Zeo-tR:	GGGTGCTGAACTTTTCTCCGTC	
3	Dnmt3a-22-F:	GCAAAGTGAGGACCATTACCACCA	
	Dnmt3a-UTR-R:	CTGATCAGGCTAGAGACAACCAAAG	

annotation and the P value. Cytoscape software was used to visualize the network results.

Construction of *Dnmt3a*^{R878H/WT}*Mx1Cre*⁺ mice

Dnmt3a R878H conditional knock-in mice were generated through recombineering by targeting PL253 vectors, as previously reported (23). Polymerase chain reaction (PCR) analysis was performed with specific primers (Table 1) to detect the genotype of the offspring. Next, we activated the mutant *Dnmt3a* protein by intraperitoneal injection with pIpC 4 weeks after birth. The mice were bred based on animal care standards, and all operations were approved by the Committee on Animal Use for Research at the Shanghai Jiao Tong University School of Medicine (23). All experiments were performed following guidelines and regulations of the Shanghai Jiao Tong University School of Medicine, China.

RNA-sequence

RNA was extracted from the bone marrow cells of *Dnmt3a*^{R878H/WT}*Mx1Cre*⁺ and *Dnmt3a*^{WT/WT}*Mx1Cre*⁺ mice using the standard protocol of TRIzol-isopropanol precipitation. The libraries were prepared according to the manufacturer's instructions (Illumina's TruSeq RNA Sample Preparation Kit, version 2) as follows:

- ❖ Step 1. Magnetic oligo-dT was utilized for pulling down the poly-A RNA from the bulk RNA of mice;
- ❖ Step 2. mRNA was segmented by metal-ion-catalyzed hydrolysis;
- ❖ Step 3. cDNA was synthesized for a-tailing and subsequent ligation of adapters.

The quality of samples was examined using a 2100

Bioanalyzer and then sequenced by Illumina MiSeq with a 200-bp paired-end. All the experiments were performed by colleagues at the Shanghai Institute of Hematology, Rui-Jin hospital of Shanghai Jiao Tong University School of Medicine.

Prediction of lncRNA

The Cuffcomparison method was used to compare Cufflinks splicing results without reference to annotations, and unknown annotations were obtained. To match the new transcripts and extract (i, u, x), 3 types of transcripts for prediction of lncRNA, we achieved the following parameters:

- ❖ Step 1. Transcription length ≥ 200 bp and exon ≥ 2 ;
- ❖ Step 2. Predicted ORF < 300 bp;
- ❖ Step 3. Pfam, CPC, and CNCI prediction—the intersection of the prediction results. A CPC score < 0 and CNCI score < 0 were selected, with Pfam being significantly higher than that of other transcripts as potential lncRNA;
- ❖ Step 4. By comparing with unknown lncRNA, the same sequence of unknown lncRNA was removed.
 - i: A transfrag falling entirely within a reference intron;
 - u: Unknown, intergenic transcript;
 - x: Exonic overlap with reference on the opposite strand.

Prediction of lncRNA target genes

Trans-regulation and cis-regulation were used to predict target genes. We chose genes with a distance of less than 10 kb without lncRNA as the target gene for cis regulation. Trans-prediction uses a murine mRNA database. The blast was used to select the complementary analogous sequence,

RNA plex (24) was used to calculate the complementary energy between the 2 sequences, and the sequences above the threshold were selected for further analysis.

OncoLnc and CCLE analysis

OncoLnc is a comprehensive interactive web server that contains the gene expression data of tumors and normal samples from the TCGA projects. The patients were divided into 2 groups according to the median expression of candidate genes. Next, we used Kaplan-Meier and log-rank methods to analyze the overall survival by the OncoLnc dataset (<http://www.oncolnc.org/>). The expression data of cell lines with DNMT3A mutation with/without NPM1 mutation was analyzed using the Broad Institute Cancer Cell Line Encyclopedia (CCLE) dataset.

Statistical analysis

The experiment was carried out in triplicate. The data for each sample was statistically analyzed using GraphPad Prism 8.0 (GraphPad Software Inc., San Diego, CA, USA). The P value was calculated by comparison of means (t-test).

Results

Genetic landscape of DNMT3A in acute myeloid leukemia

It is widely recognized that *DNMT3A* plays an important role in hematopoiesis and tumorigenesis. To explore the genetic landscape of DNMT3A in AML, we analyzed the DNMT3A alterations using cBioPortal for acute myeloid leukemia (OHSU, Nature 2018) and found that DNMT3A was altered in 114 samples from 531 patients with AML (21%). Among the DNMT3A alterations, the majority were missense mutations (putative driver, R882) and truncating mutations (putative driver) (*Figure 1A*). The genetic landscape also contained 1 unknown significant inframe mutation (Q573_A575del) and 15 missense mutations with unknown significance, including G543C, N879D, G543D, R309G, V657M, L3440, V657M, F751L, V716D, N879D, R659H, K826M, G570E, R326C, and F755S. The European Leukemia Net (ELN) risk classification (European leukemia net, 2017) and the mutation spectra of these AML patients were exhibited in *Figure 1A*. The

mutation count of DNMT3A in patients for these 4 different mutation types was also displayed (*Figure 1B*). Then, the detailed cancer types with DNMT3A alterations were further analyzed. Among all these different types, the AML type with mutated NPM1 contained the most mutations, with a nearly 50% (47.65%) alteration frequency. The second and third types of AML were acute monoblastic/monocytic leukemia (26.67%) and AML NOS (26.58%), respectively. A certain percentage of DNMT3A alterations occurred in AML with RUNX1-RUNX1T1 (18.18%), therapy-related myeloid neoplasms (16.67%), AML with myelodysplasia-related changes (10.94%), AML with biallelic mutations of CEBPA (9.09%), AML with minimal differentiation (7.69%), AML with CFBF-MYH11 (7.14%), APL with PML-RARA (5.88%), and AML with recurrent genetic abnormalities (0%) (*Figure 1C*).

Construction of the *Dnmt3a* R878H mouse model

DNMT3A consists of 3 main domains: the PWWP domain, the ADD domain, and the C-terminal catalytic domain, with the vast majority of mutations occurring mainly in the C-terminal catalytic domain (*Figure 2A*). To further explore the functional mechanism of the putative driver missense mutation DNMT3A-R882H, we used a mouse model that was reported previously to express the mutant *Dnmt3a* R878H through Cre-mediated splicing endogenously. Mice with an IFN-inducible Mx1 promoter (Mx1Cre), which is specifically expressed in the hematopoietic system, were crossed with *Dnmt3a* mutant mice, and then we used pIpC to replace the endogenous *Dnmt3a* exon 23 and induce the expression of *Dnmt3a* R878H (*Figure 2B*). Finally, we used the *Dnmt3a*^{R878H/WT}Mx1-Cre⁺ mice and *Dnmt3a*^{WT/WT}Mx1-Cre⁺ mice for further functional analysis (*Figure 2C*).

RNA-sequence of *Dnmt3a* R878H mice

To explore the function of the DNMT3A mutation in mice in detail, we performed RNA-seq of the BM cells of *Dnmt3a*^{R878H/WT}Mx1-Cre⁺ mice and *Dnmt3a*^{WT/WT}Mx1-Cre⁺ mice ON Miseq. TopHat's spliced mapping algorithm was applied to map the genome of pre-processed reads. The covering distribution of the genome in each individual sample was obtained from a 1K window. The outermost

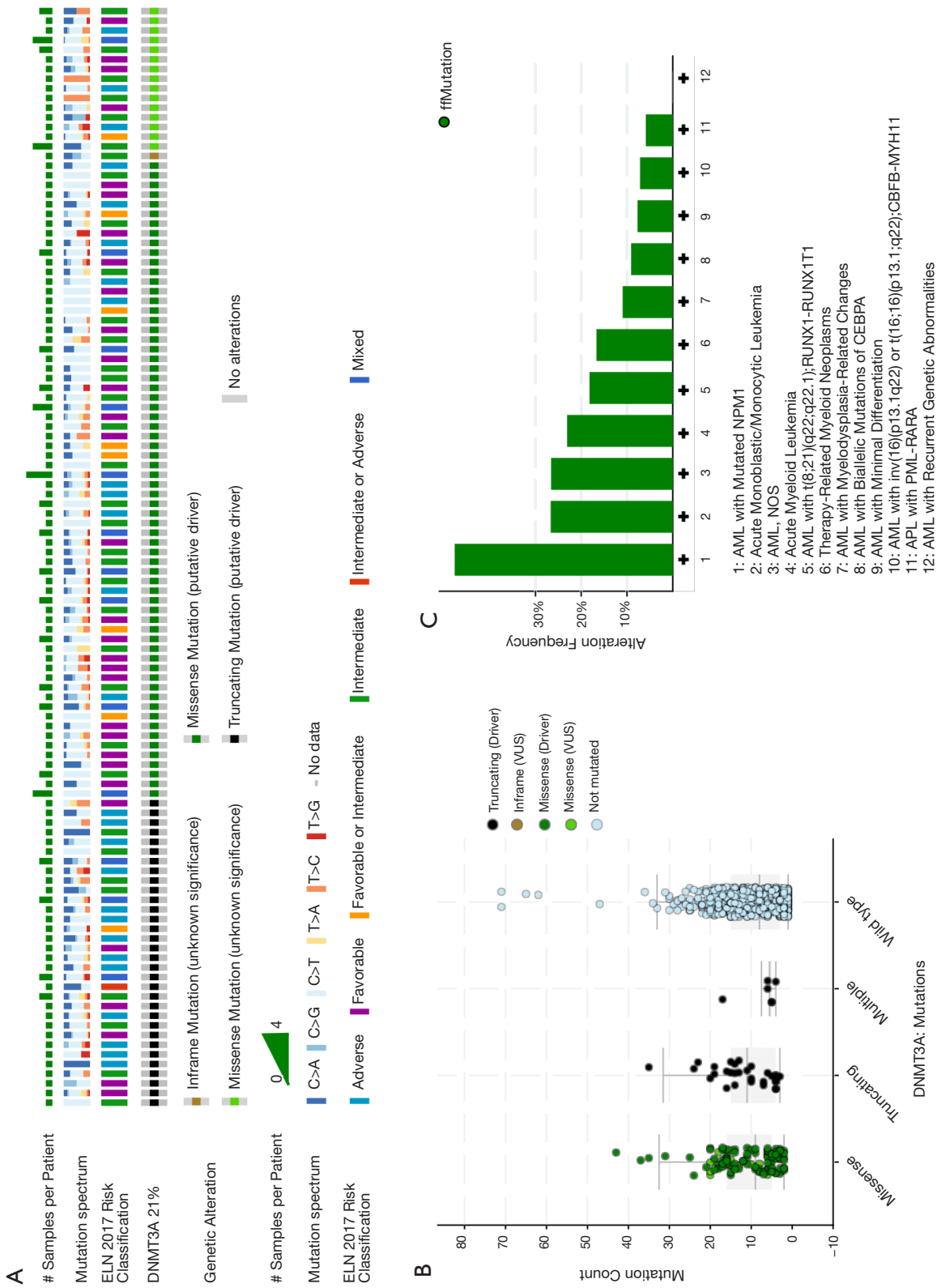


Figure 1 Genetic Landscape of DNMT3A in AML. (A) Landscape of DNMT3A alterations in AML. (B) Alteration frequency of DNMT3A in different types of AML. (C) The mutation counts of DNMT3A alterations in AML.

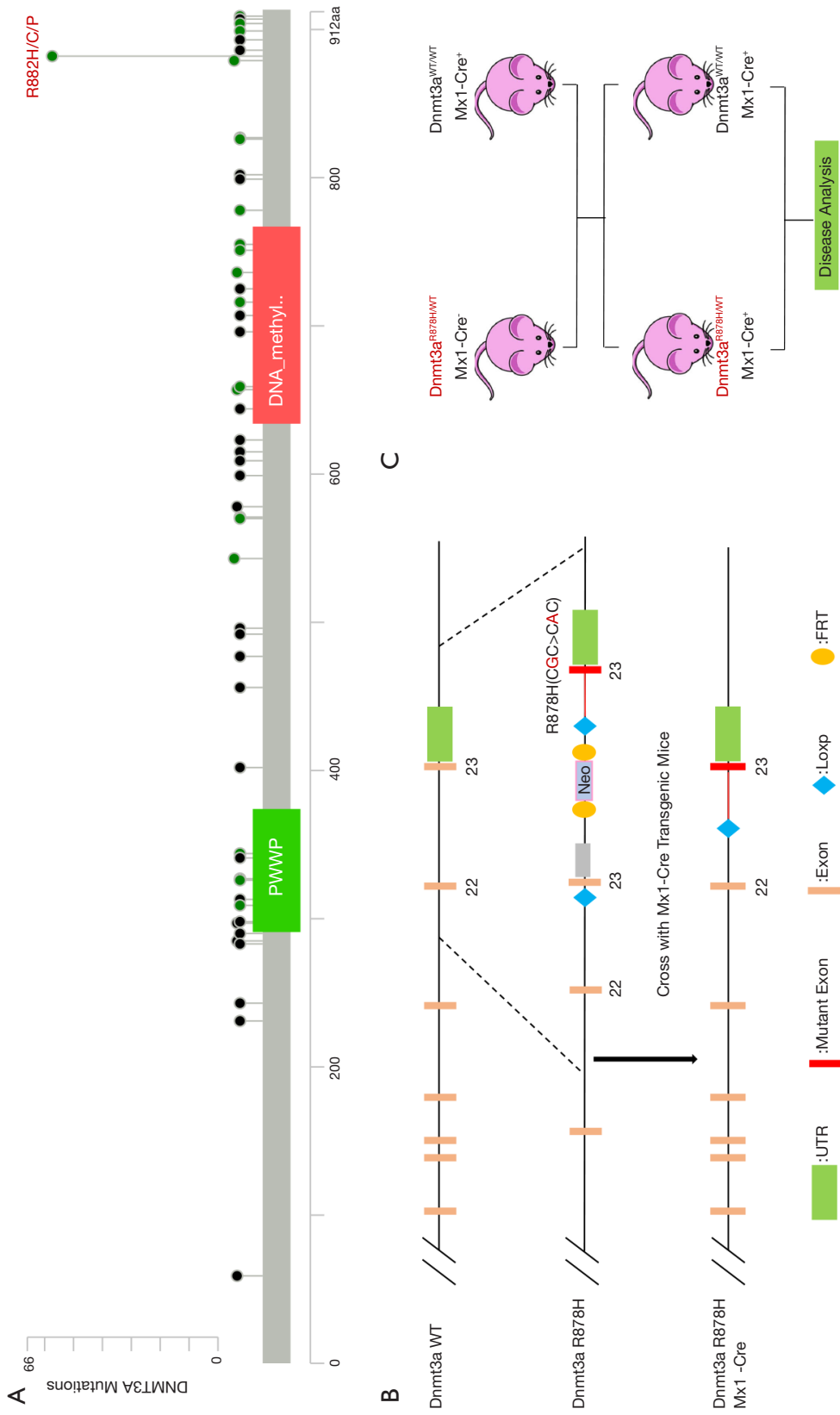


Figure 2 Schematic representation of the murine *Dnmt3a* locus. (A) Natural variants of DNMT3A in AML. (B) Schematic representation of the *Dnmt3a* R878H mouse model. (C) Diagram of the breeding of *Dnmt3a*^{R878H/WT}Mx1-Cre⁺ mice.

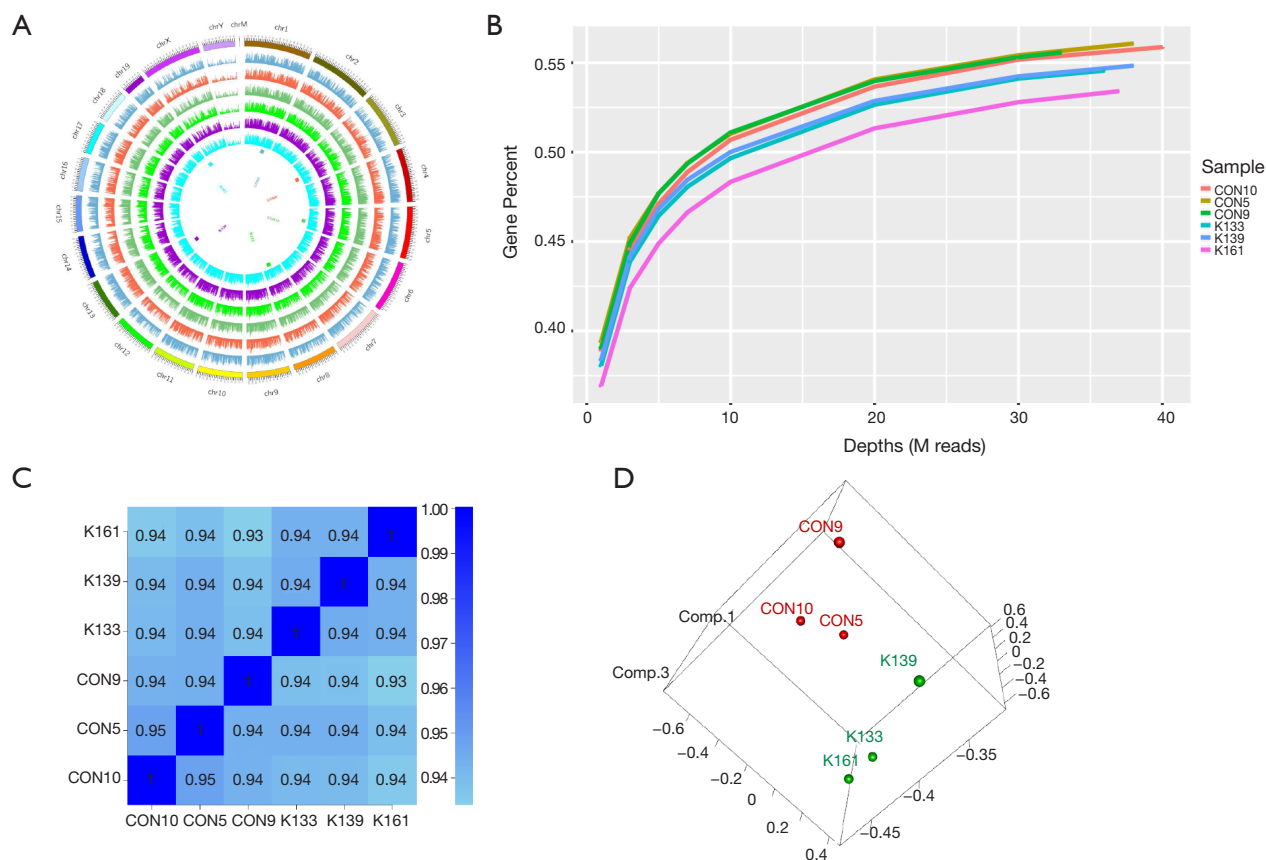


Figure 3 RNA-seq of *Dnmt3a* R878H mice. (A) Genome coverage map of RNA-seq data of *Dnmt3a*^{R878H/WT}*Mx1-Cre*⁺ mice and *Dnmt3a*^{WT/WT}*Mx1-Cre*⁺ mice. (B) Saturation cryptanalysis to detect the amount of sequenced data. (C) Heatmap map of gene expression correlation, the numerical value refers to the correlation coefficient. (D) Sample PCA map based on gene expression of *Dnmt3a*^{R878H/WT}*Mx1-Cre*⁺ mice and *Dnmt3a*^{WT/WT}*Mx1-Cre*⁺ mice.

circle in the graph in *Figure 3* is the genome, and each circle in the graph represents the chromosome coverage of a sample (*Figure 3A*). Satisfaction analysis displayed that the number of genes detected increased with the increase in sequencing (*Figure 3B*). To compare the gene expression levels between different genes and different samples, reads of sequences were transformed into fragments per kilobase of the exon model per million mapped reads (FPKM) to standardize the gene expression levels. Next, we checked the relationship between samples using the correlation coefficient (*Figure 3C*) and principal component analysis (*Figure 3D*). Both these methods demonstrated that the similarity between the murine samples was high, with correlation coefficients being over 0.9, indicating the experimental reliability and rationality of the sample

selection.

Prediction of new lncRNAs by RNA-Seq in mice

Numerous studies have shown that lncRNA plays an important role in tumorigenesis and development by regulating gene expression through chromatin modification and transcriptional regulation. In our study, Cuffcomparison was used to compare the splicing results of Cufflinks without reference to annotations, and new transcripts with unknown annotation matching were obtained. Three types of transcripts (i, u, x) were extracted to predict the lncRNAs. Then, we used the Perl script to find the corresponding gene on the chromosome of the new lncRNAs (*Figure 4A*). In addition, we compared the structure of the lncRNAs with

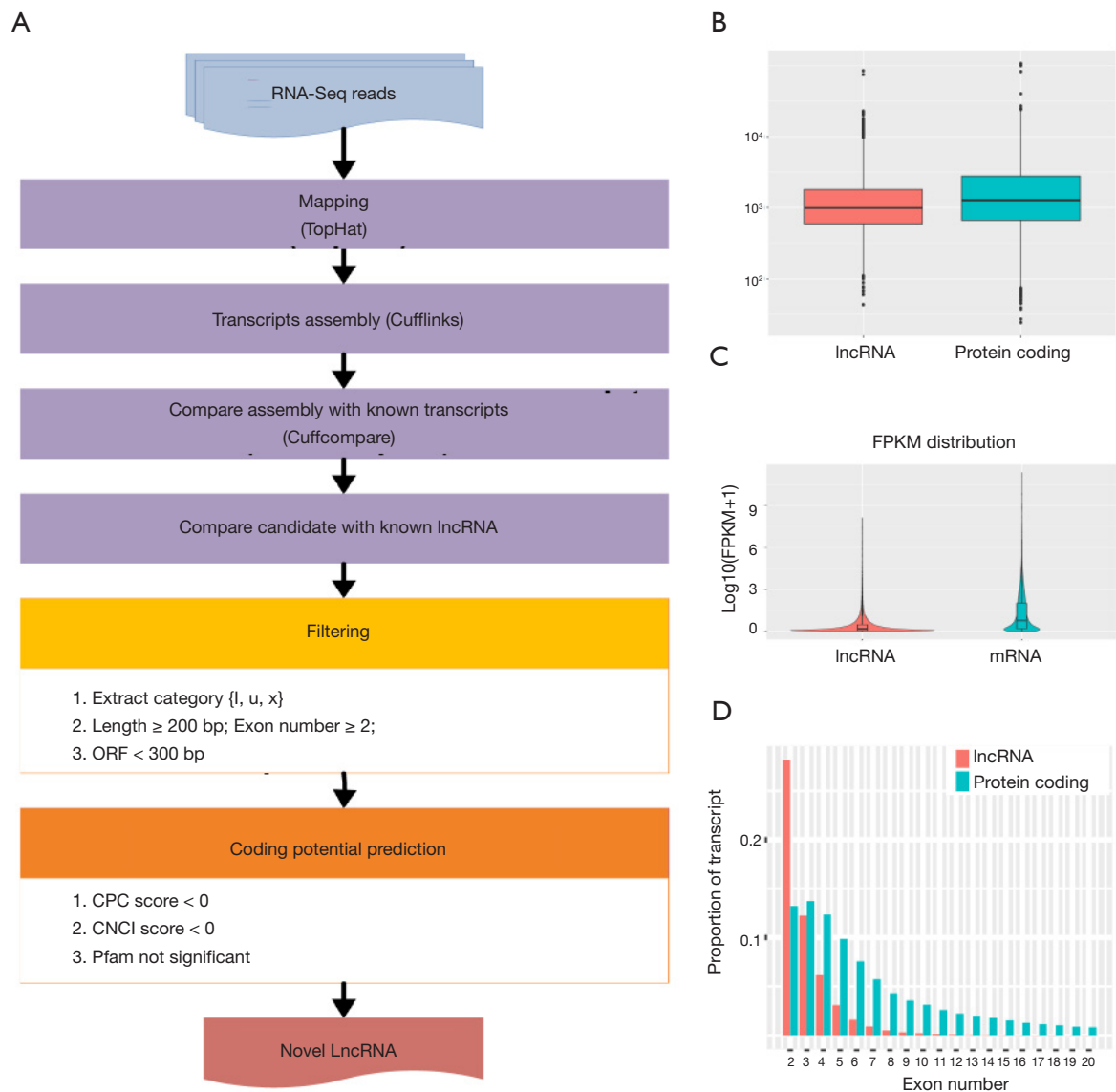


Figure 4 Prediction of new lncRNA in *Dnmt3a* R878H mice. (A) New lncRNA prediction process. (B) Length distribution of lncRNA and mRNA. (C) Comparison of exon numbers of lncRNA and mRNA. (D) Comparison of expression levels of lncRNA and mRNA.

that of the RNA. We observed no significant difference in transcription length (Figure 4B), exon number (Figure 4C), or expression level (Figure 4D) between the lncRNAs and RNAs.

We further used Cuffdiff to analyze differential lncRNAs among samples and identified 23 differentially expressed lncRNAs in *Dnmt3a*^{R878H/WT}Mx1-Cre⁺ mice (Figure 5A and Table S1). The expression of these differentially expressed lncRNAs was shown using the expression value of the

samples and the P values, as shown in Figure 5B and Table S1. The trans-regulation and cis-regulation systems were used to predict the target genes regulated by differential lncRNAs of the *Dnmt3a* mutation. In total, we found 11 candidate genes through the cis-regulation system and 113 target genes through the trans-regulation system (Figure 5C). Next, we examined differences in the expression levels of these candidate genes between *Dnmt3a*^{R878H/WT}Mx1-Cre⁺ mice and *Dnmt3a*^{WT/WT}Mx1-Cre⁺ mice. EdgeR was used

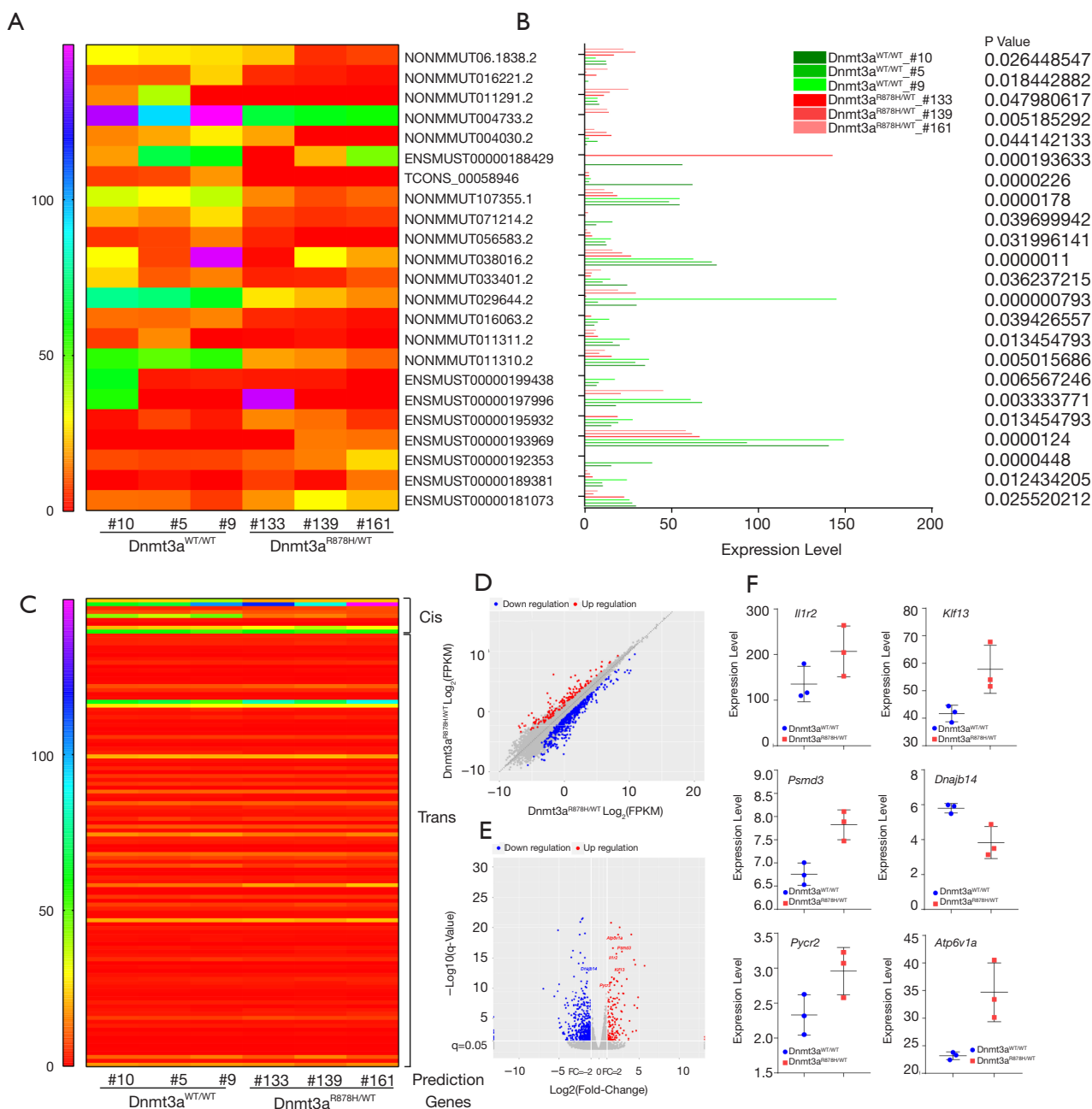


Figure 5 Prediction of candidate genes in *Dnmt3a* R878H mice. (A) Heatmap map of predicted new lncRNAs in *Dnmt3a*^{R878H/WT}*Mx1-Cre*⁺ mice and *Dnmt3a*^{WT/WT}*Mx1-Cre*⁺ mice. (B) The expression levels of these lncRNAs. P value was displayed on the right side of the figure. (C) Heatmap map of candidate genes expressed in *Dnmt3a*^{R878H/WT}*Mx1-Cre*⁺ mice and *Dnmt3a*^{WT/WT}*Mx1-Cre*⁺ mice by cis and trans regulation. (D) Express correlation scatter plot of RNA-seq. (E) Differential Gene Volcano Map. Red indicates up-regulation of differentially expressed genes and blue indicates down-regulation of differentially expressed genes. (F) The expression levels of candidate genes of *Dnmt3a*^{R878H/WT}*Mx1-Cre*⁺ mice and *Dnmt3a*^{WT/WT}*Mx1-Cre*⁺ mice.

to analyze the different genes among the samples and obtain the correction of the P value posterior multiple hypothesis tests. We then determined the P value threshold by controlling the false discovery rate (FDR). The scatter map of gene expression (*Figure 5D*) and the volcanic map of the differential genes (*Figure 5E*) showed the up-regulated genes (red plot) and down-regulated genes (green plot) in *Dnmt3a*^{R878H/WT}Mx1-Cre⁺ mice compared with *Dnmt3a*^{WT/WT}Mx1-Cre⁺ mice. Next, the prognostic values of these candidate genes were analyzed through the OncoLnc dataset, and 13 genes were found to be closely related to the prognosis of AML (*Tables S2,S3*). Taken together, the results above indicate that only 6 genes were both differentially expressed in *Dnmt3a*^{R878H/WT}Cre⁺ mice and associated with the prognosis of AML. Therefore, we chose only these 6 genes among the predicted candidate genes. The expressions of these differentially expressed candidate genes were further validated using the expression value of the murine samples (*Figure 5F*).

Prognosis and functional analysis of candidate genes in AML

We then explored the efficiency of these candidate genes in the survival of patients with AML. OncoLnc tools were used to analyze the survival of patients with AML. The Kaplan-Meier curve and log-rank test analyses revealed that increased *IL1R2* (P=0.0022), *KLF13* (P=0.0134), *ATP6V1A* (P=0.0295), *PSMD3* (P=0.0165), and *PYCR2* (P=0.0211) mRNA levels were significantly associated with poor prognosis in terms of overall survival (OS) of AML patients (*Figure 6A*). Decreased Dnaj heat shock protein family (Hsp40) member B14 (*DNAJB14*) mRNA levels also had a tendency to indicate a poor prognosis, with P=0.0126. Next, we chose two cell lines OCI-AML3 (harboring DNMT3A R882C mutation and NPM1 mutation) and OCI-AML2 (harboring DNMT3A R635W mutation) and attempted to explore the expression level of these dysregulated genes in human AML patients cell lines with NPM1 and/or DNMT3A mutations. The results based on CCLE showed that most of these dysregulated genes showed greater expression in OCI-AML3 cells compared with OCI-AML2 cells (*Figure 6B*). Functional analysis of these target genes was performed using Metascape tools, and the significant terms

were identified and then hierarchically clustered into a tree based on κ -statistical similarities (*Figure 6C,D, Table 2*).

Discussion

DNMT3A gene mutations occur in a variety of hematopoietic diseases. The mutation rate in adult AML is more than 20%, and 10–15% in myelodysplastic syndrome (MDS). The loss of *DNMT3A* was clinically observed to be associated with a variety of hematological malignancies (25–27). However, the detailed mechanism of leukemogenesis associated with DNMT3A mutations was not clear.

Increasing evidence has shown that lncRNAs can promote or inhibit the growth of tumors by regulating or maintaining gene expression. Abnormal expression of lncRNA often leads to the occurrence, development, and metastasis of tumors (18). It has been reported that HOX antisense intergenic RNA (HOTAIR) exhibits a significant positive correlation with DNMT3A (28). The lncRNA H19 plays a crucial role in the initiation and progression of cancers, while the overexpression of H19 in AML patients has a strong positive association with DNMT3A mutations. Patients with a high expression level of H19 have shown a lower complete remission (CR) rate compared with those patients with low expression (29). Furthermore, the molecular dynamics analysis of lncRNA demonstrated that some lncRNAs could integrate with the promoter of the 5'-UTR and recruit DNMT3A protein. The complex could then methylate the target genes, leading to epigenetic alternation (30). In this study, we focused on those lncRNAs related to hematological tumors to fully understand the mechanism of these lncRNAs in diseases; we hope our findings will lead to new ideas for the research, diagnosis, and prognosis of hematological tumors.

To further explore those lncRNAs regulated by *DNMT3A* mutations, we used the *DNMT3A* mutation conditional knock-in mice for correlation analysis. We analyzed the RNA-seq data using a special algorithm, detailed in section 2.4 of this article. Our data showed that considerable differences exist in gene expression and lncRNA expression between *DNMT3A*-mutant mice and wild mice. In addition, mutant mice showed significant heterogeneity compared with wild mice, which is consistent with previous reports (23). Twenty-three *Dnmt3a* mutation-specific lncRNAs were identified, 14 of which were novel lncRNAs and 9 of which were known lncRNAs in the database of murine lncRNAs. To explore the expression level of these lncRNAs in human AML, we checked the

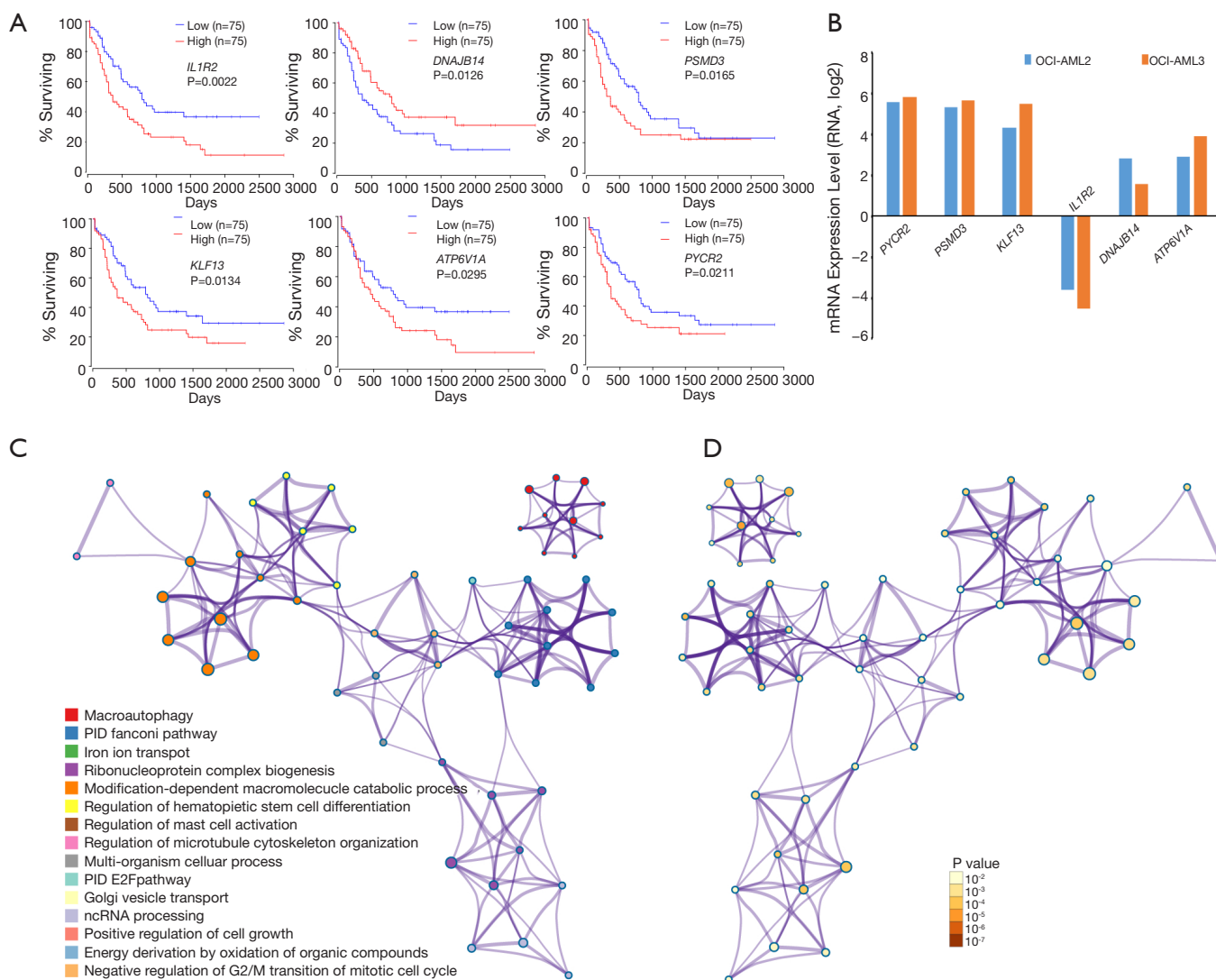


Figure 6 Prognosis and functional analysis of these candidate genes in Dnmt3a R878H mice. (A) The prognostic values of the predicted genes regulated by these lncRNAs in Dnmt3a^{R878H/AVT} Mx1-Cre⁺ mice and Dnmt3a^{WT/WT} Mx1-Cre⁺ mice. (B) The expression level of the six candidate genes in OCI-AML3 cells and OCI-AML2 cells based on the CCLE dataset. The significant terms among the candidate genes (metascape) according to its functional term (C) and P value (D).

homologous lncRNAs by comparing the ID or whole-genome pairwise alignment (hg19/mm10, genome.UCSC.edu) of these lncRNAs in murine and human samples. Meanwhile, because of the rapid evolution and highly non-conservative characteristics of lncRNA, we were unable to match the murine lncRNAs with human lncRNAs, which prevented us from comprehensively evaluating the expression of these lncRNAs in databases in human AML patients (31).

According to this finding, we identified the differentially

expressed lncRNAs in Dnmt3a mutant mice and predicted their downstream target genes based on cis- and trans-regulation. Indeed, more than 6 genes, including *Il1r2*, *Klf13*, *Psm3*, *Dnajb14*, *Pycr2*, and *Atp6v1a*, were aberrantly regulated by the DNMT3A R878H mutation and suggested a poor prognosis. The functional analysis demonstrated that these genes are associated with macro-autophagy, iron ion transport, hematopoietic stem cell differentiation, and the cell cycle, which are, in turn, closely related to the occurrence and development of hematological malignancies.

Table 2 Ontology pathway analysis of targetable genes

GO	Category	Description	Count	%	Log10(P)	Log10(q)
GO:0016236	GO Biological Processes	Macroautophagy	8	8.16	-4.51	-0.38
M1	Canonical Pathways	PID FANCONI PATHWAY	4	4.08	-4.4	-0.38
GO:0006826	GO Biological Processes	Iron ion transport	4	4.08	-3.87	-0.36
GO:0042273	GO Biological Processes	Ribosomal large subunit biogenesis	4	4.08	-3.7	-0.36
GO:1902036	GO Biological Processes	Regulation of hematopoietic stem cell differentiation	4	4.08	-3.67	-0.36
GO:0043632	GO Biological Processes	Modification-dependent macromolecule catabolic process	10	10.2	-3.56	-0.36
GO:0034660	GO Biological Processes	ncRNA metabolic process	9	9.18	-3.32	-0.3
GO:0030307	GO Biological Processes	Positive regulation of cell growth	5	5.1	-3.2	-0.26
GO:0033003	GO Biological Processes	Regulation of mast cell activation	3	3.06	-3.09	-0.22
GO:0070507	GO Biological Processes	Regulation of microtubule cytoskeleton organization	5	5.1	-3.01	-0.22
GO:0044764	GO Biological Processes	Multi-organism cellular process	3	3.06	-3.01	-0.22
M40	Canonical Pathways	PID E2F PATHWAY	3	3.06	-2.47	0
GO:0048193	GO Biological Processes	Golgi vesicle transport	6	6.12	-2.37	0
GO:0016482	GO Biological Processes	Cytosolic transport	4	4.08	-2.36	0
GO:0015980	GO Biological Processes	Energy derivation by oxidation of organic compounds	5	5.1	-2.21	0
GO:0010972	GO Biological Processes	Negative regulation of G2/M transition of mitotic cell cycle	3	3.06	-2.19	0

Consistent with our result, the immune microenvironment-related gene, *IL1R2*, is known to be associated with a poor prognosis of AML and lung cancer in TCGA and Gene Expression Omnibus (GEO) datasets (32,33). In addition, a hormone-sensitive patient-derived xenograft (PDX) model showed that Krüppel-like factor 1 (*KLF1*) was related to the hormone sensitivity in acute lymphoblastic leukemia (34). *ATP6V1A* was a critical gene related to autophagy, which can induce autophagy through binding with a small-molecule compound EN6 and activating the mTOR signaling pathway (35). *PSMD* is considered an important cancer-related gene in the NF- κ B pathway, which was shown to be consistently activated in Sezary Syndrome (36). Furthermore, some studies indicate that the single-nucleotide polymorphism (SNP) variations of *PSMD3* in European individuals are related to the number of immune cells in peripheral blood and inflammatory diseases such as asthma (37). However, the roles of *PYCR2* and *DNAJB12* in hematopoietic malignancies have not been widely studied, although *PYCR2* has been associated with proteomic subgrouping and reported to be involved in metabolic reprogramming of hepatocellular carcinoma with hepatitis B infection (38). As an ER J-protein, *DNAJB14* accelerates

the degradation of membrane proteins to maintain homeostasis (39). Our study is the first to report that the decreased expression of *DNAJB14* is associated with the poor prognosis of AML.

Conclusions

In conclusion, we found the specific lncRNAs regulated by *DNMT3A* mutations using a DNMT3A R878H knock-in mouse model and predicted the candidate genes influenced by these lncRNAs. These findings might provide information relevant to the future development of novel therapeutics targeting these special lncRNAs and candidate genes for *DNMT3A*-mutated leukemic cells.

Acknowledgments

We would like to thank Editage for their English language editing services. We specially thank all of our colleagues at Shanghai Institute of Hematology for constructing the animal model and technical help.

Funding: This work was supported by the National Natural

Science Foundation of China [Grant number 81570151], Shanghai Municipal Education Commission-Gaofeng Clinical Medicine [Grant number 20152507].

Footnote

Conflicts of Interest: The authors have no conflicts of interest to declare.

Ethical Statement: The authors are accountable for all aspects of the work in ensuring that questions related to the accuracy or integrity of any part of the work are appropriately investigated and resolved. All experiments were performed following guidelines and regulations of the Shanghai Jiao Tong University School of Medicine, China.

Open Access Statement: This is an Open Access article distributed in accordance with the Creative Commons Attribution-NonCommercial-NoDerivs 4.0 International License (CC BY-NC-ND 4.0), which permits the non-commercial replication and distribution of the article with the strict proviso that no changes or edits are made and the original work is properly cited (including links to both the formal publication through the relevant DOI and the license). See: <https://creativecommons.org/licenses/by-nc-nd/4.0/>.

References

1. Yan XJ, Xu J, Gu ZH, et al. Exome sequencing identifies somatic mutations of DNA methyltransferase gene DNMT3A in acute monocytic leukemia. *Nat Genet* 2011;43:309-15.
2. Linch DC, Hills RK, Burnett AK, et al. The clinical impact of mutant DNMT3A R882 variant allele frequency in acute myeloid leukaemia. *Br J Haematol* 2020. [Epub ahead of print].
3. Ostronoff F, Othus M, Lazenby M, et al. Prognostic significance of NPM1 mutations in the absence of FLT3-internal tandem duplication in older patients with acute myeloid leukemia: a SWOG and UK National Cancer Research Institute/Medical Research Council report. *J Clin Oncol* 2015;33:1157-64.
4. Schnittger S, Haferlach C, Alpermann T, et al. DNMT3A is a Powerful Follow-up Marker in NPM1 mutated AML. *Blood* 2014;124.
5. Bezerra MF, Lima AS, Pique-Borras MR, et al. Co-occurrence of DNMT3A, NPM1, FLT3 mutations identifies a subset of acute myeloid leukemia with adverse prognosis. *Blood* 2020. [Epub ahead of print].
6. Cappelli LV, Meggendorfer M, Dicker F, et al. DNMT3A mutations are over-represented in young adults with NPM1 mutated AML and prompt a distinct co-mutational pattern. *Leukemia* 2019;33:2741-6.
7. Noh KM, Wang H, Kim HR, et al. Engineering of a Histone-Recognition Domain in Dnmt3a Alters the Epigenetic Landscape and Phenotypic Features of Mouse ESCs. *Mol Cell* 2018;69:533.
8. Weinberg DN, Papillon-Cavanagh S, Chen H, et al. The histone mark H3K36me2 recruits DNMT3A and shapes the intergenic DNA methylation landscape. *Nature* 2019;573:281-6.
9. Challen GA, Sun D, Jeong M, et al. Dnmt3a is essential for hematopoietic stem cell differentiation. *Nat Genet* 2011;44:23-31.
10. Zhang X, Su J, Jeong M, et al. DNMT3A and TET2 compete and cooperate to repress lineage-specific transcription factors in hematopoietic stem cells. *Nat Genet* 2016;48:1014-23.
11. Sanders MA, Chew E, Flensburg C, et al. MBD4 guards against methylation damage and germ line deficiency predisposes to clonal hematopoiesis and early-onset AML. *Blood* 2018;132:1526-34.
12. Gu T, Lin X, Cullen SM, et al. DNMT3A and TET1 cooperate to regulate promoter epigenetic landscapes in mouse embryonic stem cells. *Genome Biol* 2018;19:88.
13. Ketkar S, Verdoni AM, Smith AM, et al. Remethylation of Dnmt3a (-/-) hematopoietic cells is associated with partial correction of gene dysregulation and reduced myeloid skewing. *Proc Natl Acad Sci U S A* 2020;117:3123-34.
14. Yang L, Rodriguez B, Mayle A, et al. DNMT3A Loss Drives Enhancer Hypomethylation in FLT3-ITD-Associated Leukemias. *Cancer Cell* 2016;30:363-5.
15. Zhang X, Wang X, Wang XQD, et al. Dnmt3a loss and Idh2 neomorphic mutations mutually potentiate malignant hematopoiesis. *Blood* 2020. [Epub ahead of print].
16. Lu R, Wang J, Ren Z, et al. A Model System for Studying the DNMT3A Hotspot Mutation (DNMT3A(R882)) Demonstrates a Causal Relationship between Its Dominant-Negative Effect and Leukemogenesis. *Cancer Res* 2019;79:3583-94.
17. Trimarchi T, Bilal E, Ntziachristos P, et al. Genome-wide mapping and characterization of Notch-regulated long noncoding RNAs in acute leukemia. *Cell* 2014;158:593-606.
18. Garzon R, Volinia S, Papaioannou D, et al. Expression and prognostic impact of lncRNAs in acute myeloid leukemia.

- Proc Natl Acad Sci U S A 2014;111:18679-84.
19. Hughes JM, Salvatori B, Giorgi FM, et al. CEBPA-regulated lncRNAs, new players in the study of acute myeloid leukemia. *J Hematol Oncol* 2014;7:69.
 20. Zeng C, Xu Y, Xu L, et al. Inhibition of long non-coding RNA NEAT1 impairs myeloid differentiation in acute promyelocytic leukemia cells. *BMC Cancer* 2014;14:693.
 21. Tsai CH, Yao CY, Tien FM, et al. Incorporation of long non-coding RNA expression profile in the 2017 ELN risk classification can improve prognostic prediction of acute myeloid leukemia patients. *EBioMedicine* 2019;40:240-50.
 22. Li Q, Dong C, Cui J, et al. Over-expressed lncRNA HOTAIRM1 promotes tumor growth and invasion through up-regulating HOXA1 and sequestering G9a/EZH2/Dnmts away from the HOXA1 gene in glioblastoma multiforme. *J Exp Clin Cancer Res* 2018;37:265.
 23. Dai YJ, Wang YY, Huang JY, et al. Conditional knockin of Dnmt3a R878H initiates acute myeloid leukemia with mTOR pathway involvement. *Proc Natl Acad Sci U S A* 2017;114:5237-42.
 24. Tafer H, Hofacker IL. RNAplex: a fast tool for RNARNA interaction search. *Bioinformatics* 2008;24:2657-63.
 25. Shlush LI, Zandi S, Mitchell A, et al. Identification of pre-leukaemic haematopoietic stem cells in acute leukaemia. *Nature* 2014;506:328-33.
 26. Bond J, Touzart A, Lepretre S, et al. DNMT3A mutation is associated with increased age and adverse outcome in adult T-cell acute lymphoblastic leukemia. *Haematologica* 2019;104:1617-25.
 27. Bartels S, Faisal M, Busche G, et al. Mutations associated with age-related clonal hematopoiesis in PMF patients with rapid progression to myelofibrosis. *Leukemia* 2019. [Epub ahead of print].
 28. Zhang YY, Huang SH, Zhou HR, et al. Role of HOTAIR in the diagnosis and prognosis of acute leukemia. *Oncol Rep* 2016;36:3113-22.
 29. Zhang TJ, Zhou JD, Zhang W, et al. H19 overexpression promotes leukemogenesis and predicts unfavorable prognosis in acute myeloid leukemia. *Clin Epigenetics* 2018;10:47.
 30. Lister N, Shevchenko G, Walshe JL, et al. The molecular dynamics of long noncoding RNA control of transcription in PTEN and its pseudogene. *Proc Natl Acad Sci U S A* 2017;114:9942-7.
 31. Jiang YY, Zhu H, Zhang H. [Analysis of orthologous lncRNAs in humans and mice and their species-specific epigenetic target genes]. *Nan Fang Yi Ke Da Xue Xue Bao* 2018;38:731-5.
 32. Guo X, Zhang Y, Zheng L, et al. Global characterization of T cells in non-small-cell lung cancer by single-cell sequencing. *Nat Med* 2018;24:978-85.
 33. Yan H, Qu J, Cao W, et al. Identification of prognostic genes in the acute myeloid leukemia immune microenvironment based on TCGA data analysis. *Cancer Immunol Immunother* 2019;68:1971-8.
 34. Jing D, Bhadri VA, Beck D, et al. Opposing regulation of BIM and BCL2 controls glucocorticoid-induced apoptosis of pediatric acute lymphoblastic leukemia cells. *Blood* 2015;125:273-83.
 35. Chung CY, Shin HR, Berdan CA, et al. Covalent targeting of the vacuolar H(+)-ATPase activates autophagy via mTORC1 inhibition. *Nat Chem Biol* 2019;15:776-85.
 36. Caprini E, Cristofolini C, Arcelli D, et al. Identification of key regions and genes important in the pathogenesis of Sezary syndrome by combining genomic and expression microarrays. *Cancer Res* 2009;69:8438-46.
 37. Crosslin DR, McDavid A, Weston N, et al. Genetic variants associated with the white blood cell count in 13,923 subjects in the eMERGE Network. *Hum Genet* 2012;131:639-52.
 38. Gao Q, Zhu H, Dong L, et al. Integrated Proteogenomic Characterization of HBV-Related Hepatocellular Carcinoma. *Cell* 2019;179:561-77.e22.
 39. Goodwin EC, Motamedi N, Lipovsky A, et al. Expression of DNAJB12 or DNAJB14 causes coordinate invasion of the nucleus by membranes associated with a novel nuclear pore structure. *PLoS One* 2014;9:e94322.

Cite this article as: Dai YJ, Hu F, He SY, Wang YY. Epigenetic landscape analysis of lncRNAs in acute myeloid leukemia with DNMT3A mutations. *Ann Transl Med* 2020;8(6):318. doi: 10.21037/atm.2020.02.143

Supplementary

Table S1 List of the 23 differentially express lncRNAs in mice

lncRNA_id	Locus	length	Mutant_FPKM	WT_FPKM	Fold_change-KI/WT	P value	Up/down regulate	CON10_FPKM	CON5_FPKM	CON9_FPKM	K133_FPKM	K139_FPKM	K161_FPKM	g1_FPKM	g2_FPKM	CON10_count	CON5_count	CON9_count	K133_count	K139_count	K161_count	g1_count	g2_count
ENSMUST00000181073	10:12916645-12923127	1060	11.9628	27.8584	0.42941447	0.025520212	DOWN	29.8609	27.6539	26.0603	23.0123	5.25344	7.62281	27.8584	11.9628	319.79	291.639	281.947	247.042	56.1092	80.6764	297.792	127.943
ENSMUST00000189381	11:120961748-120998295	778	3.2643	15.1341	0.21569172	0.012434205	DOWN	10.6107	10.3084	24.483	4.8182	3.27893	1.69577	15.1341	3.2643	111.903	106.111	253.58	50.3003	34.4239	17.7718	157.198	34.1653
ENSMUST00000192353	9:90863158-90863307	149	0.00001	18.2156	5.49E-07	4.48E-05	DOWN	15.5194	39.1274	0	0	0	0	18.2156	0	0.924815	1.87793	0	0	0	0	0.93425	0
ENSMUST00000193969	1:40028765-40125231	3071	62.3625	128.128	0.48672031	1.24E-05	DOWN	140.934	93.7948	149.654	66.5196	62.0561	58.512	128.128	62.3625	4698.99	3169.95	4825.37	2252.53	2058.92	1958.84	4231.44	2090.1
ENSMUST00000195932	5:64563770-64563919	149	6.4096	20.9937	0.30531064	0.013454793	DOWN	15.5194	19.5637	27.8981	19.2288	0	0	20.9937	6.4096	0.924815	0.938967	1.22502	1.00604	0	0	1.0296	0.335347
ENSMUST00000197996	3:116818814-116818978	164	22.184	49.1212	0.45161763	0.003333771	DOWN	18.2222	67.8826	61.2588	0	21.0801	45.4718	49.1212	22.184	1.84963	5.6338	4.9001	0	1.86075	3.94928	4.12784	1.93668
ENSMUST00000199438	5:55652948-55653147	199	0.00001	10.9683	9.12E-07	0.006567246	DOWN	7.09008	8.27617	17.5385	0	0	0	10.9683	0	1.84963	1.87793	3.67507	0	0	0	2.46755	0
NONMMUT011310.2	11:86811827-86816129	2697	12.0495	33.8983	0.3554603	0.005015686	DOWN	34.9619	29.4028	37.3302	15.7349	8.57	11.8437	33.8983	12.0495	1126.28	964.28	1131.36	522.471	273.5	385.052	1073.97	393.674
NONMMUT011311.2	11:86811827-86816129	3365	6.65937	20.9716	0.3175423	0.013454793	DOWN	20.4244	16.3869	26.1035	7.84417	5.48907	6.64488	20.9716	6.65937	827.858	669.522	1024.68	322.604	220.53	269.542	840.687	270.892
NONMMUT016063.2	12:113418557-113422730	324	1.31627	9.26689	0.1420401	0.039426557	DOWN	5.79041	7.68822	14.322	3.9485	0.000212	0.0001025	9.26689	1.31627	10.4099	12.9279	23.9053	6.84833	0.0003674	0.0001744	15.7477	2.28296
NONMMUT029644.2	17:39842994-40064883	1005	16.7226	61.1403	0.27351191	7.93E-07	DOWN	30.1526	7.82938	145.439	1.00478	29.7146	19.4483	61.1403	16.7226	250.677	63.767	1262.64	8.21912	248.042	159.929	525.695	138.73
NONMMUT033401.2	19:3065710-3197782	3793	5.88141	16.7959	0.35016939	0.036237215	DOWN	24.7823	10.6023	15.003	3.78238	4.24366	9.61817	16.7959	5.88141	1162.49	504.222	673.729	182.084	197.239	455.154	780.148	278.159
NONMMUT038016.2	2:75637800-75658998	471	21.6525	70.9167	0.30532301	1.10E-06	DOWN	76.3101	73.5892	62.8507	26.9847	21.7723	16.2004	70.9167	21.6525	303.339	284.507	238.88	105.634	84.6642	63.1885	275.575	84.4957
NONMMUT056583.2	6:41198232-41201843	682	3.18951	13.4708	0.23677213	0.031996141	DOWN	12.8745	12.2037	15.3341	4.5013	3.4721	1.59512	13.4708	3.18951	76.884	72.9559	86.4559	27.4114	20.5385	9.48349	78.7653	19.1444
NONMMUT071214.2	9:114728980-114749343	1249	0.938233	7.69172	0.12197961	0.039699942	DOWN	6.9036	16.171	0.0005742	0.697771	2.09962	0.0173108	7.69172	0.938233	80.2104	190.673	0.0064346	8.28162	24.2203	0.201633	90.2965	10.9012
NONMMUT107355.1	2:75637800-75658998	5126	15.6662	52.9073	0.29610659	1.78E-05	DOWN	54.9198	48.8492	54.9529	19.0106	16.4787	11.5092	52.9073	15.6662	3307.24	2975.07	3198.28	1163.95	985.535	695.047	3160.19	948.177
TCONS_00058946	18:16274551-16275002	203	1.81432	22.9585	0.07902607	2.26E-05	DOWN	62.3655	2.80515	3.7048	2.80804	2.63491	0	22.9585	1.81432	24.0452	0.938967	1.22502	1.00604	0.930376	0	8.73639	0.645472
ENSMUST00000188429	2:158353699-158361581	132	47.7206	18.8542	2.53103287	0.000193633	UP	56.5625	0	0	143.162	0	0	18.8542	47.7206	0.87376	0	0	1.94146	0	0	0.291253	0.647153
NONMMUT004030.2	1:180326969-180424802	287	11.4343	3.96384	2.88465226	0.044142133	UP	1.43995	7.64303	2.80855	15.655	12.8714	5.77661	3.96384	11.4343	1.57312	7.85032	2.67088	16.8598	13.291	5.99372	4.03144	12.0482
NONMMUT004733.2	10:12916645-12923127	1089	9.08173	0.00473866	1916.51859	0.005185292	UP	0.0064683	0.0053452	0.0024025	0.0050926	14.1075	13.1326	0.0047387	9.08173	0.0710552	0.0580466	0.02677090	0.0560715	155.368	143.174	0.0519576	99.5327
NONMMUT011291.2	11:86583864-86683836	2239	17.125	7.93494	2.15817637	0.047980617	UP	8.64975	7.50489	7.65018	11.2771	14.7008	25.3971	7.93494	17.125	167.089	148.753	142.345	222.645	283.868	494.349	152.729	333.621
NONMMUT016221.2	13:3538074-3611108	217	7.16486	0.778304	9.20573452	0.018442882	UP	1.984E-05	2.33489	0	6.98086	1.11135	13.4024	0.778304	7.16486	6.599E-06	0.703692	0	2.20444	0.334686	4.04543	0.234566	2.19485
NONMMUT061838.2	7:63886350-63938915	1319	23.0638	10.62	2.17173258	0.026448547	UP	12.8185	12.451	6.59051	17.0542	29.53	22.6073	10.62	23.0638	170.574	166.09	86.1292	226.306	392.291	298.178	140.931	305.592

Table S2 The predict targetable genes by Cis regulation

chr	Start	End	Strands	lncRNA_id	chr	Start	End	Strands	Gene_id	Gene_name	Oncolnc (P value)
1	40088510	40091581	+	ENSMUST00000193969	1	40085984	40102436	+	ENSMUSG00000026073	Il1r2	0.0022
7	63886352	63887671	-	NONMMUT061838.2	7	63886350	63938915	-	ENSMUSG00000052040	Klf13	0.0134
11	86584695	86586934	-	NONMMUT011291.2	11	86585019	86586994	-	ENSMUSG00000018171	Vmp1	0.0179
11	120963843	120964764	+	ENSMUST00000189381	11	120955225	120956231	+	ENSMUSG00000025161	Slc16a3	0.0395
13	3566035	3566252	-	NONMMUT016221.2	13	3566035	3611108	-	ENSMUSG00000033799	Fam208b	0.626
11	86811827	86814524	-	NONMMUT011310.2	11	86799586	86807039	-	ENSMUSG00000018425	Dhx40	0.792
11	86812764	86816129	-	NONMMUT011311.2	11	86799586	86807039	-	ENSMUSG00000018425	Dhx40	0.792
9	114748094	114749343	+	NONMMUT071214.2	9	114756836	114781993	-	ENSMUSG00000032436	Cmtm7	0.981
1	180424511	180424798	+	NONMMUT004030.2	1	180432386	180483467	-	ENSMUSG00000053963	6330403A02Rik	NA
12	113420741	113421065	-	NONMMUT016063.2	12	113418557	113422730	-	ENSMUSG00000076617	Ighm	NA
6	41198232	41198914	-	NONMMUT056583.2	6	41202754	41203044	+	ENSMUSG00000076477	Trbv21	NA

Table S3 The predict targetable genes by Trans regulation

lncRNA_id	Trans_Target_mRNA	Trans_Target_gene	gene_name	Trans_Evalue	Oncolnc (P value)
NONMMUT107355.1	ENSMUST00000085826	ENSMUSG00000020661	Dnmt3a	-87.7	0.000353
ENSMUST00000181073	ENSMUST00000131158	ENSMUSG00000022438	Parvb	-71.8	0.000404
ENSMUST00000181073	ENSMUST00000090178	ENSMUSG00000074212	Dnajb14	-82.4	0.0126
ENSMUST00000181073	ENSMUST00000138549	ENSMUSG00000025817	Nudt5	-73.2	0.0164
NONMMUT107355.1	ENSMUST00000152102	ENSMUSG00000017221	Psmc3	-92.8	0.0165
ENSMUST00000181073	ENSMUST00000194253	ENSMUSG00000026520	Pycr2	-71	0.0211
ENSMUST00000181073	ENSMUST00000130036	ENSMUSG00000052459	Atp6v1a	-76.1	0.0295
ENSMUST00000181073	ENSMUST0000041203	ENSMUSG00000030270	Cpne9	-68.3	0.0352
NONMMUT107355.1	ENSMUST00000022036	ENSMUSG00000021553	Slc28a3	-90.7	0.05
NONMMUT107355.1	ENSMUST00000127090	ENSMUSG00000020823	Sec14i1	-90.1	0.0549
ENSMUST00000181073	ENSMUST00000127660	ENSMUSG00000052738	Suclg1	-79.1	0.0552
ENSMUST00000181073	ENSMUST00000144378	ENSMUSG00000029655	N4bp2l2	-74.6	0.0572
ENSMUST00000181073	ENSMUST00000140370	ENSMUSG00000038324	Trpc4ap	-75.4	0.0627
ENSMUST00000181073	ENSMUST00000110549	ENSMUSG00000042817	Fit3	-74.1	0.0629
ENSMUST00000181073	ENSMUST00000147183	ENSMUSG00000052326	Rbbp4	-79.2	0.082
NONMMUT107355.1	ENSMUST00000127211	ENSMUSG00000027787	Nmd3	-90.2	0.0957
ENSMUST00000181073	ENSMUST00000127373	ENSMUSG00000025173	Wdr45b	-73.9	0.114
ENSMUST00000181073	ENSMUST00000112311	ENSMUSG00000025825	Iscu	-75.7	0.118
NONMMUT107355.1	ENSMUST00000156046	ENSMUSG00000020526	Znhit3	-92	0.122
ENSMUST00000181073	ENSMUST00000099374	ENSMUSG00000074802	Gas2l3	-74.8	0.145
ENSMUST00000181073	ENSMUST00000123641	ENSMUSG00000006191	Cdkal1	-77.5	0.146
ENSMUST00000181073	ENSMUST00000091674	ENSMUSG00000006191	Cdkal1	-68.2	0.146
ENSMUST00000181073	ENSMUST00000023867	ENSMUSG00000023104	Rfc2	-80.6	0.162
ENSMUST00000181073	ENSMUST00000135018	ENSMUSG00000024773	Atg2a	-77.1	0.167
ENSMUST00000181073	ENSMUST00000135943	ENSMUSG00000031604	Msmo1	-71.2	0.173
ENSMUST00000181073	ENSMUST00000159426	ENSMUSG00000036636	Cln7	-74.2	0.177
ENSMUST00000181073	ENSMUST00000123133	ENSMUSG00000058498	Rnf207	-73.6	0.192
ENSMUST00000181073	ENSMUST00000196258	ENSMUSG00000045482	Trrap	-81.5	0.196
ENSMUST00000181073	ENSMUST00000202421	ENSMUSG00000053134	Supt7l	-84.2	0.207
ENSMUST00000181073	ENSMUST00000181042	ENSMUSG00000037416	Dmxi1	-80.8	0.222
ENSMUST00000181073	ENSMUST00000116231	ENSMUSG00000080115	Mettl21b	-69.5	0.223
ENSMUST00000181073	ENSMUST00000188847	ENSMUSG00000048874	Phf3	-84.5	0.229
NONMMUT107355.1	ENSMUST00000203625	ENSMUSG00000001521	Tulp3	-91	0.254
ENSMUST00000181073	ENSMUST00000202627	ENSMUSG00000029161	Cgref1	-83	0.263
ENSMUST00000181073	ENSMUST00000160708	ENSMUSG00000004626	Sbxp2	-75	0.263
ENSMUST00000181073	ENSMUST00000140279	ENSMUSG00000014504	Srp19	-77.2	0.267
ENSMUST00000181073	ENSMUST00000186398	ENSMUSG00000026356	Dars	-64.7	0.282
ENSMUST00000181073	ENSMUST00000153173	ENSMUSG00000030869	Ndufab1	-74.7	0.296
ENSMUST00000181073	ENSMUST00000138468	ENSMUSG00000027598	Itch	-77.3	0.303
ENSMUST00000181073	ENSMUST00000186246	ENSMUSG00000067336	Bmpr2	-76.2	0.304
NONMMUT107355.1	ENSMUST00000134323	ENSMUSG00000035949	Fbxw2	-86	0.306
ENSMUST00000181073	ENSMUST0000040519	ENSMUSG00000037787	Apopt1	-78.4	0.313
ENSMUST00000181073	ENSMUST00000163992	ENSMUSG00000015316	Slamf1	-79.8	0.313
ENSMUST00000181073	ENSMUST00000192890	ENSMUSG00000026705	Klhl20	-75.1	0.345
NONMMUT107355.1	ENSMUST00000146104	ENSMUSG00000007570	Fance	-89.2	0.372
ENSMUST00000181073	ENSMUST00000108249	ENSMUSG00000037643	Prkci	-77.7	0.377
NONMMUT107355.1	ENSMUST00000153924	ENSMUSG00000007371	Btbd19	-90.9	0.39
ENSMUST00000181073	ENSMUST00000071852	ENSMUSG00000056941	Commd7	-82	0.393
ENSMUST00000181073	ENSMUST00000173966	ENSMUSG00000002984	Tomm40	-78.9	0.396
NONMMUT107355.1	ENSMUST00000141152	ENSMUSG00000047126	Cltc	-86.1	0.401
ENSMUST00000181073	ENSMUST00000146233	ENSMUSG00000040483	Xaf1	-72.3	0.415
ENSMUST00000181073	ENSMUST00000128582	ENSMUSG00000039768	Dnajc11	-72.5	0.421
ENSMUST00000181073	ENSMUST00000142327	ENSMUSG00000003660	Snmp200	-78.3	0.456
ENSMUST00000181073	ENSMUST00000195731	ENSMUSG00000026080	Chst10	-75.8	0.469
ENSMUST00000181073	ENSMUST00000185401	ENSMUSG00000053877	Srcap	-74.9	0.485
ENSMUST00000181073	ENSMUST00000206479	ENSMUSG00000053158	Fes	-82.3	0.504
ENSMUST00000181073	ENSMUST00000211173	ENSMUSG00000020818	Mfsd11	-65.5	0.531
ENSMUST00000181073	ENSMUST00000084926	ENSMUSG00000044037	Als2cl	-76.8	0.538
ENSMUST00000181073	ENSMUST00000154704	ENSMUSG00000041966	Dcaf17	-72.2	0.552
NONMMUT107355.1	ENSMUST00000162792	ENSMUSG00000033400	Ag1	-90	0.566
ENSMUST00000181073	ENSMUST00000086353	ENSMUSG00000040528	Milr1	-71.1	0.587
ENSMUST00000181073	ENSMUST00000134594	ENSMUSG00000001143	Lman2l	-76.4	0.593
ENSMUST00000181073	ENSMUST00000202151	ENSMUSG00000036435	Exoc1	-72.1	0.604
ENSMUST00000181073	ENSMUST00000127536	ENSMUSG00000037214	Thap1	-80.4	0.605
ENSMUST00000181073	ENSMUST00000186061	ENSMUSG00000032409	Atr	-81.9	0.612
ENSMUST00000181073	ENSMUST00000182970	ENSMUSG00000029110	Rnf4	-75.3	0.636
ENSMUST00000181073	ENSMUST00000198325	ENSMUSG00000001016	Ilf2	-78	0.676
ENSMUST00000181073	ENSMUST00000029786	ENSMUSG00000028140	Mrp19	-73	0.692
ENSMUST00000181073	ENSMUST00000180554	ENSMUSG00000037926	Ssh2	-67.2	0.702
ENSMUST00000181073	ENSMUST00000197394	ENSMUSG00000022160	Mettl3	-69.8	0.741
ENSMUST00000181073	ENSMUST00000118679	ENSMUSG00000022498	Txndc11	-83.3	0.758
ENSMUST00000181073	ENSMUST00000200029	ENSMUSG00000032480	Dhx30	-75.2	0.763
NONMMUT107355.1	ENSMUST00000152751	ENSMUSG00000027115	Kif18a	-92.1	0.794
ENSMUST00000181073	ENSMUST00000038474	ENSMUSG00000039356	Exosc2	-78.8	0.803
NONMMUT107355.1	ENSMUST00000182164	ENSMUSG00000024073	Birc6	-92.3	0.814
NONMMUT107355.1	ENSMUST00000153936	ENSMUSG00000029578	Wipi2	-91.4	0.817
NONMMUT107355.1	ENSMUST0000027036	ENSMUSG00000025903	Lypla1	-91.3	0.829
ENSMUST00000181073	ENSMUST00000036194	ENSMUSG00000040121	Rep15	-77.6	0.876
ENSMUST00000181073	ENSMUST00000150946	ENSMUSG00000006058	Snf8	-83.4	0.887
ENSMUST00000181073	ENSMUST00000044158	ENSMUSG00000041560	Gltscr2	-77.4	0.899
ENSMUST00000181073	ENSMUST00000144696	ENSMUSG00000027282	Mtch2	-82.8	0.901
NONMMUT107355.1	ENSMUST00000174852	ENSMUSG00000021418	Rpp40	-91.5	0.922
ENSMUST00000181073	ENSMUST00000034392	ENSMUSG00000031917	Nip7	-71.7	0.928
NONMMUT107355.1	ENSMUST00000141208	ENSMUSG00000020220	Vps13d	-92.4	0.945
ENSMUST00000181073	ENSMUST00000204594	ENSMUSG00000025758	Plk4	-72.9	0.96
NONMMUT107355.1	ENSMUST00000155824	ENSMUSG00000071866	Ppia	-87.3	0.963
ENSMUST00000181073	ENSMUST00000126755	ENSMUSG00000024008	Cpne5	-78.6	0.965
ENSMUST00000181073	ENSMUST00000186897	ENSMUSG00000032555	Topbp1	-81	0.992
NONMMUT107355.1	ENSMUST00000143616	ENSMUSG00000026798	Coq4	-85.5	0.993
ENSMUST00000181073	ENSMUST00000145614	ENSMUSG00000037740	Mrps26	-72.8	0.994
ENSMUST00000181073	ENSMUST00000160484	ENSMUSG00000033400	Ag1	-76.7	0.566 (Ag1)
ENSMUST00000181073	ENSMUST00000161808	ENSMUSG00000015961	Adcs	-78.5	6.78e10-6
ENSMUST00000181073	ENSMUST0000021135	ENSMUSG00000020783	120014J11Rik	-80.2	NA
ENSMUST00000181073	ENSMUST00000145859	ENSMUSG00000074578	150012F01Rik	-73.7	NA
ENSMUST00000181073	ENSMUST00000132778	ENSMUSG00000078584	AU022252	-68.8	NA
ENSMUST00000181073	ENSMUST00000194220	ENSMUSG00000033488	BC026585	-80.1	NA
ENSMUST00000181073	ENSMUST00000053033	ENSMUSG00000044768	D1Erd622e	-74	NA
ENSMUST00000181073	ENSMUST00000202707	ENSMUSG00000038456	Dennd2a	-84	NA
NONMMUT107355.1	ENSMUST00000060894	ENSMUSG00000044726	Erich5	-90.6	NA
ENSMUST00000181073	ENSMUST00000060009	ENSMUSG00000048647	Exd1	-75.6	NA
ENSMUST00000181073	ENSMUST00000206754	ENSMUSG00000046826	Fam187b	-83.7	NA
ENSMUST00000181073	ENSMUST00000118793	ENSMUSG00000081650	Gm16181	-78.7	NA
ENSMUST00000181073	ENSMUST00000185926	ENSMUSG00000096036	Gm21778	-81.1	NA
ENSMUST00000181073	ENSMUST00000194153	ENSMUSG00000034837	Gnat1	-74.3	NA
ENSMUST00000181073	ENSMUST00000198518	ENSMUSG00000067242	Lgi1	-68.1	NA
ENSMUST00000181073	ENSMUST00000132185	ENSMUSG00000020691	Mettl2	-74.4	NA
ENSMUST00000181073	ENSMUST00000178684	ENSMUSG00000020072	Pbid2	-70.1	NA
ENSMUST00000181073	ENSMUST00000126347	ENSMUSG00000032289	Thsd4	-73.8	NA
ENSMUST00000181073	ENSMUST00000049778	ENSMUSG00000051034	Zfp11	-76.9	NA
ENSMUST00000181073	ENSMUST00000075916	ENSMUSG00000029587	Zfp12	-83.5	NA
ENSMUST00000181073	ENSMUST00000168691	ENSMUSG00000025602	Zfp202	-80.5	NA
ENSMUST00000181073	ENSMUST00000108336	ENSMUSG00000037640	Zfp60	-76	NA
ENSMUST00000181073	ENSMUST00000108212	ENSMUSG00000059975	Zfp74	-70.8	NA